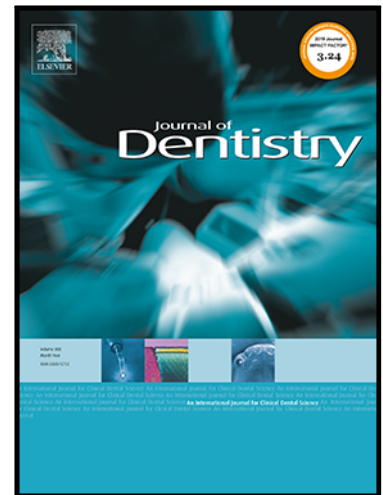


## Journal Pre-proof

Trueness and precision of combined healing abutment-scan body system depending on the scan pattern and implant location: an in-vitro study

Mustafa Borga Donmez , Gülce Çakmak , Sevda Atalay , Hakan Yilmaz , Burak Yilmaz

PII: S0300-5712(22)00225-1  
DOI: <https://doi.org/10.1016/j.jdent.2022.104169>  
Reference: JJOD 104169



To appear in: *Journal of Dentistry*

Received date: 9 February 2022  
Revised date: 17 May 2022  
Accepted date: 31 May 2022

Please cite this article as: Mustafa Borga Donmez , Gülce Çakmak , Sevda Atalay , Hakan Yilmaz , Burak Yilmaz , Trueness and precision of combined healing abutment-scan body system depending on the scan pattern and implant location: an in-vitro study, *Journal of Dentistry* (2022), doi: <https://doi.org/10.1016/j.jdent.2022.104169>

This is a PDF file of an article that has undergone enhancements after acceptance, such as the addition of a cover page and metadata, and formatting for readability, but it is not yet the definitive version of record. This version will undergo additional copyediting, typesetting and review before it is published in its final form, but we are providing this version to give early visibility of the article. Please note that, during the production process, errors may be discovered which could affect the content, and all legal disclaimers that apply to the journal pertain.

© 2022 Published by Elsevier Ltd.

**Trueness and precision of combined healing abutment-scan body system depending on the scan pattern and implant location: an in-vitro study**

Original article

Full Title: Trueness and precision of combined healing abutment-scan body system depending on the scan pattern and implant location: an in-vitro study

Short title: Effect of scan pattern and implant location on scan accuracy

Authors: Mustafa Borga Donmez, DDS, PhD,<sup>a,b</sup> Gülce Çakmak DDS, PhD,<sup>c</sup> Sevda Atalay, DDS, PhD,<sup>d</sup> Hakan Yilmaz DDS, MSc,<sup>e</sup> and Burak Yilmaz DDS, PhD<sup>f,g,h</sup>

<sup>a</sup>Visiting Researcher, Department of Reconstructive Dentistry and Gerodontology, School of Dental Medicine, University of Bern, Bern, Switzerland; mustafa-borga.doenmez@zmk.unibe.ch

<sup>b</sup>Assistant Professor, Department of Prosthodontics, Faculty of Dentistry, Istinye University, İstanbul, Turkey.

<sup>c</sup>Buser Foundation Scholar for Implant Dentistry, Department of Reconstructive Dentistry and Gerodontology, School of Dental Medicine, University of Bern, Bern, Switzerland; guelce.cakmak@zmk.unibe.ch

<sup>d</sup>Prosthodontist, Private Practice, İstanbul, Turkey; sevda.atalay@gmail.com

<sup>e</sup>Orthodontist, Private Practice, İstanbul, Turkey; hakanyilmaz90@gmail.com

<sup>f</sup>Associate Professor, Department of Reconstructive Dentistry and Gerodontology, School of Dental Medicine, University of Bern, Bern, Switzerland

<sup>g</sup>Associate Professor, Department of Restorative, Preventive and Pediatric Dentistry, School of Dental Medicine, University of Bern, Bern, Switzerland; burak.yilmaz@zmk.unibe.ch

<sup>h</sup>Adjunct Professor, Division of Restorative and Prosthetic Dentistry, The Ohio State University College of Dentistry, Ohio, USA.

Corresponding author:

Dr Mustafa Borga Dönmez

Department of Reconstructive Dentistry and Gerodontology

School of Dental Medicine, University of Bern

Freiburgstrasse 7, 3010, Bern

SWITZERLAND

Email: mustafa-borga.doenmez@zmk.unibe.ch

**Keywords:** accuracy, combined healing abutment-scan body, implant position, scan pattern

## HIGHLIGHTS

1. Scan pattern and implant location affected scan accuracy.
2. Greater scan area and complex movements resulted in higher deviations.
3. Implant located at central incisor site showed the highest trueness.

## ABSTRACT

**Objective:** To test the effect of scan pattern and the location of the implant on the trueness and precision of implant scans when the combined healing abutment-scan body (CHA-SB) system is used.

**Material and Methods:** A partially edentulous maxillary model with CHA-SBs secured on implants at 3 different sites in the left quadrant (central incisor, first premolar, and first molar) was fabricated. The model was scanned with an industrial light scanner to generate a master reference model (MRM) file. An intraoral scanner (TRIOS 3) was used to perform the test scans (n=8) with 4 different scan patterns (SP1, SP2, SP3, and SP4) with an intraoral scanner. The test scans were superimposed over the MRM file with a metrology software to calculate the distance deviations of the CHA-SB system. Data were analyzed with a 2-way analysis of variance and Tukey's honestly significant difference tests for accuracy ( $\alpha=.05$ ).

**Results:** Trueness ( $P=.001$ ) and precision ( $P=.018$ ) were significantly affected by the interaction between the scan pattern and implant location. The implant located at the central incisor site ( $56.7 \pm 35.9$ ,  $36.2 \pm 18.6$ ) had higher trueness than that of located at the premolar site ( $94.1 \pm 20.4$ ,  $100.3 \pm 20$ ) when SP2 ( $P=.037$ ) and SP4 ( $P=.002$ ) were used. The implant at the molar site ( $71.9 \pm 25.7$ ,  $147.2 \pm 49.7$ ) had trueness either similar to (when SP2 was used,  $P \geq .276$ ) or lower than (when SP4 was used,  $P \leq .024$ ) those of others. Scans of the central incisor and premolar implants had the lowest trueness when scanned with SP1 ( $P \leq .009$ ), while the scans of molar implant showed higher trueness when performed by using SP2 and SP3 when compared with SP4 ( $P \leq .005$ ). When SP4 was used, the implant at the molar site had lower precision ( $43 \pm 18.9$ ) than the implants located at the central incisor ( $14.1 \pm 11$ ) and premolar sites ( $15.4 \pm 11.3$ ) ( $P=.002$ ). Scan patterns affected the scan precision of central incisor implant ( $P=.009$ ), as SP4 ( $14.1 \pm 11$ ) led to a higher precision than SP1 ( $47.7 \pm 27$ ) ( $P=.006$ ).

**Conclusions:** The scan accuracy of combined healing abutment-scan body system was affected by scan pattern and implant location. SP1, which involved palatal and rotational scans resulted in the lowest trueness for central incisor and premolar implants, while the scans of the central incisor implant showed the highest trueness among different sites when SP4 was used. However,

the scan pattern and implant site had a minor effect on precision. Scan precision at different implant sites only differed when SP4 was used, which resulted in the lowest precision for molar implant.

### **Clinical Significance**

Rotational scanning of the palate after linear scanning of complete arch did not have any additional benefit for accuracy. In addition, rotational movements could impair the scan accuracy at the molar site.

## **1. INTRODUCTION**

Intraoral scanners (IOSs) have started to succeed conventional impressions [1] as the tendency towards using IOSs for implant-supported restorations is increasing [2, 3]. IOSs, laboratory scanners, and scan bodies (SBs) can be used for the digitization of implants either in a direct or indirect digital workflow [4]. The conventional impression is digitized by using laboratory scanners and laboratory SBs in indirect workflow. However, in direct workflow intra oral SBs are scanned by using an IOS for data acquisition [5]. Thus, any potential errors related to the clinical and laboratory phases are minimized as the impression trays and the impression materials are eliminated [6-9].

The usage of SBs has improved significantly since they were first introduced and there are various SB designs, as nearly all major manufacturers as well as dental laboratories and third parties are offering these components [9]. However, most of the available SBs and healing abutments (HAs) have cylindrical or conical shapes [4, 9, 10], which have been a major problem in implant prosthodontics [11, 12]. Thus, an interim implant-supported crown or a custom HA is necessary to contour the emergence profile, especially in the anterior region or for molar crowns

with wide cervical areas [10]. Nevertheless, these solutions still pose a problem as for the acquisition of the soft tissue the HA or the interim crown has to be removed, which may interrupt the soft tissue healing during the replacement of parts. A recently introduced combined healing abutment-scan body (CHA-SB) system eliminates this problem. The anatomical contour is formed by the polyetheretherketone HA while the SB (ScanPeg; Neoss Implant System), which is medical grade acrylic resin is fitted in to the screw channel of this HA. This combined system allows the simultaneous scanning of both the implant and the contoured soft tissue [10]. The scans performed by using this system is made at the HA level, which prevent the disturbance of the healing of soft tissues.

The main concern revolving around IOSs is their accuracy [13], which is the combination of trueness and precision (UNI ISO 5725-1:2004) [4, 14]. Trueness is described as how far an object's measurements deviate from its the actual dimensions, while precision is defined as the proximity of repeated measurements [4, 15]. Even though the accuracy of IOSs have improved over time, various factors affect the accuracy of the digital scans [16]. Among these factors, the location of the implant [17-19] and the effect of the scan pattern [20, 21] are rather scarcely investigated for single implant scenarios. Moreover, to the authors' knowledge, no study has investigated the combined effect of these factors on implant scan accuracy. The authors are aware of 4 studies that evaluated the accuracy of CHA-SB system [4, 21-23]. Even though the effect of implant location [23] and scan pattern [21] has been investigated separately, the knowledge on the combined effect of these parameters on the scan accuracy of the CHA-SB system is lacking. Therefore, the present study aimed to investigate the effect of 4 different scan patterns on the scan accuracy (trueness and precision) of single implants positioned at 3 different sites when using CHA-SB system. The null hypotheses were that i) the trueness of the scans would not be

affected by scan pattern and the implant location, ii) the scan precision of the scans would not be affected by scan pattern and the implant location.

## 2. MATERIAL AND METHODS

A maxillary partially edentulous model was fabricated similar to previous studies [21-23] by using an auto-polymerizing polymethylmethacrylate resin (Weropress; Merz Dental GmbH), which is a feasible material to scan. Three implants (4.0 mm×11 mm, Neoss ProActive Straight; Neoss Implant System) were placed at left central incisor, first premolar, and first molar sites. To properly align the indexed HA, each implant was placed with an inner slot facing buccally. HAs of the CHA-SB system were then positioned in accordance with the inner slots of the implants and fixed. The SBs (ScanPeg; Neoss Implant System) were then fitted into the screw hole of the HA [4, 10, 24].

The CHA-SB system utilizes a friction-fit mechanism between the vertical groove of the HA and the outdent of the SB. This unique connection type gives the system an anti-rotational feature while ensuring the proper position of the CHA-SB assembly (Fig. 1). The parts of the CHA-SB systems were kept assembled until all test scans were completed.

An industrial blue-light scanner (ATOS Core 80 5MP; GOM GmbH) was used to generate a master reference model (MRM) in the standard tessellation language (STL) format and a metrology software (Pro 8.1; GOM GmbH) was utilized for the digitization of the data. The reference scanner uses a triangulation based stereo camera and has 1 µm probing error form, 3 µm probing error size, 5 µm sphere spacing error, and 7 µm length measurement error [25]. The surface of the MRM was coated with a thin layer (2 µm) of antireflective spray before scanning [26]. This spray layer was not altered until all scans were completed.

Four different scan patterns were tested in the present study and 8 scans were performed for each scan pattern. The test scans were performed by using an IOS with confocal microscopy technology (TRIOS 3 Cart version 1.4.7.5; 3Shape) [26, 27]. The same experienced operator (G.Ç.) who has 4 years of experience in digital implant dentistry carried out all scans and calibrations in the same temperature- (20 °C) and humidity-controlled (45%) room, in which the master reference model scan was performed. The room was lit by sunlight and the air pressure was set at  $750 \pm 5$  mm [7]. Once all MRM and SB surfaces were scanned without any flaws, the scan was deemed completed.

The scan patterns performed in the present study are as follows (Fig. 2):

**Scan Pattern 1 (SP1):** The scan started from the occlusal surface of the ipsilateral distal molar and captured the entire arch. Afterwards, the lingual surfaces of the teeth in the arch were scanned starting from the contralateral distal molar, followed by the buccal scans originating from the ipsilateral distal molar. Next, the entire arch was scanned with buccolingual rotational movements starting from the ipsilateral distal molar and the acquisition was completed with the buccolingual rotational scan of the palate.

**Scan Pattern 2 (SP2):** The occlusal, lingual, and buccal scans were similar to those of SP1. However, buccolingual rotational movements were only limited to the quadrant with the implants and the palatal scan was not performed.

**Scan Pattern 3 (SP3):** The entire arch was scanned with continuous buccolingual rotational movements starting from the ipsilateral distal molar to contralateral distal molar followed by a second scan in reverse using the same buccolingual rotational movements.

**Scan Pattern 4 (SP4):** The scan started from the occlusal aspect of the implant at the central incisor site and captured the whole quadrant with the implants by moving distally. The lingual surfaces of this quadrant were then scanned starting from the distal molar and turning buccally



around the implant at the central incisor site for buccal surface scans. After completing the buccal scan of this quadrant, the occlusal, lingual, and buccal scans of the entire arch were performed similar to the SP1.

To evaluate accuracy, test scan STL files were superimposed over the MRM STL file by using the best-fit algorithm feature of a metrology software (GOM Inspect 2018; GOM GmbH). Initial alignment was performed with the 'prealignment' feature and the errors were minimized with the 'local best fit' feature [26].

To calculate the trueness of the test scans, the mean distance deviations for each scan pattern and at implant location were measured in x, y, and z axes. Two parallel circular planes (one at the top of the SB and one 3 mm below) were created to measure the deviations in both master scan and the test scans (Fig. 3) [21-23]. The linear deviations of the center points of these 2 circles were calculated for each scan by using the following formula [17, 18, 26]:

$$3D = (\sqrt{x^2 + y^2 + z^2})$$

Prior to test scans, the fit between the SB and the HA was analyzed by superimposing the STL file of the MRM over the library file of the CHA-SB with the same method mentioned above, which allowed to evaluate the congruence between these 2 STL files (Fig. 4).

The number of scans for each scan pattern was determined according a power analysis (power: 0.80,  $\alpha$ : 0.05, and effect size: 0.6) based on the results of a previous study [26]. Normality of data was evaluated by using Shapiro-Wilk test. Trueness data were analyzed (SPSS for Windows v 25.0; IBM Corp) with 2-way analysis of variance (ANOVA) followed by the Tukey test ( $\alpha=0.05$ ). Mean values and 95% confidence limits for distance deviations (trueness and precision) were calculated for each scan pattern and implant position. The variances of deviations

were used to define precision (distance and angular deviation data) [5, 26] and variance homogeneities among SPs were compared with 2-way ANOVA and Tukey tests ( $\alpha = .05$ ).

### 3. RESULTS

The STL file of the MRM showed a maximum distance deviation of 1.2  $\mu\text{m}$  for the CHA-SB assembly at the central incisor site, 1.9  $\mu\text{m}$  for the CHA-SB assembly at the premolar site, and 1.3  $\mu\text{m}$  for the CHA-SB assembly at the molar site when superimposed over the library CAD file (Fig. 4).

Figures 5 and 6 illustrate the box-plot graphs of each scan pattern-implant location pair for trueness and precision. Table 1 shows the 2-way ANOVA results of the trueness and precision measurements. The interaction between scan pattern and implant location affected the trueness ( $P=.001$ ) and the precision ( $P=.018$ ) of the scans.

The scans of implants at different sites showed different deviations when SP2 ( $P=.045$ ) and SP4 ( $P<.001$ ) were used. For SP2, the scans of the central incisor implant had higher trueness (lower deviations) than the premolar implant ( $P=.037$ ), while the scans of the molar implant had trueness similar to that of other implant scans ( $P\geq.276$ ). For SP4, molar implant had the highest and the central incisor implant had the lowest deviations ( $P\leq.024$ ). However, no significant differences were observed among different implant locations when SP1 ( $P=.310$ ) and SP3 ( $P=.205$ ) were used. SP1 resulted in the highest deviations for the implants located at the central incisor ( $P\leq.009$ ) and premolar ( $P\leq.002$ ) locations, whereas the differences among other scan patterns were nonsignificant for both implant locations ( $P\geq.059$ ). SP4 led to higher deviations than SP2 ( $P=.003$ ) and SP3 ( $P=.005$ ) for molar implant, while SP1 resulted in similar deviations to those of other scan patterns ( $P\geq.05$ ).

Other than SP4 ( $P=.001$ ), all scan patterns resulted in similar precision among different implant locations ( $P\geq.089$ ). Molar implant had the lowest precision (highest deviations) when SP4 was used ( $P=.002$ ), whereas the difference between the central incisor and the premolar implants was nonsignificant ( $P=.981$ ). Central incisor implant had higher precision when scanned with SP4 when compared with scanning with SP1 ( $P=.006$ ), while the difference between every other scan pattern comparison was nonsignificant ( $P\geq.064$ ). Scan patterns did not affect the scan precision of the premolar ( $P\geq.369$ ) and molar ( $P\geq.068$ ) implants.

#### 4. DISCUSSION

The first and second null hypotheses of the present study were rejected as both scan patterns and implant locations affected the trueness and the precision. Among the scan patterns tested in the present study, SP3 resulted in higher accuracy for all implant locations. Even though SP1 resembles the manufacturer's recommended scan pattern for the IOS utilized in the present study when digitizing a dentate maxilla (starts with capturing the occlusal surfaces in the entire arch, then scanning the buccal and lingual surfaces, and finalizing the scan with a sweeping motion through the palate) [28], it presented the lowest trueness for the central incisor and premolar implants. This may be related to an interruption in the stitching process as SP1 captured the widest scan area with more complex movements that involved the scan of the palate and the buccolingual rotational scan of the whole arch. For the molar implant, however, the scans performed with SP4 resulted in lower trueness than the scans performed with other scan patterns. Given the scarcity of the knowledge on the effects of scan patterns on the single implant scan accuracy and the CHA-SB system, the findings of the present study need in vivo support.

To authors' knowledge, only 2 studies have investigated the effect of scan pattern on the scan accuracy of single implants [20, 21]. Yilmaz et al [21] evaluated the scan accuracy of CHA-

SB system placed at mandibular right first molar site when digitized by using different patterns, and concluded that scan patterns had no significant effect on the distance deviations (trueness and precision). In addition, the measured deviations in the present study was lower than those of Yilmaz et al's [21] study (131.8-139.1  $\mu\text{m}$ ). These contradicting results may be related to the differences in scan patterns, number of implants, and anatomy of the reference model. Motel et al [20] scanned 3 different SBs with the IOS utilized in the present study, by using either a one-step method where the ridge of the titanium model and the SBs were scanned simultaneously similar to the CHA-SB system or a two-step method where the titanium model was digitized first followed by the digitization of SBs. It was concluded that the one-step method was more accurate compared with the two-step method. The mean distance deviations reported (71  $\mu\text{m}$  for one-step scan and 125  $\mu\text{m}$  for two-step scan) are comparable with the findings of the present study (Table 2), even though the implants in Motel et al's [20] study were placed linearly in a titanium block rather than to a model.

The effect of scan pattern on the scan accuracy is not well-understood as contradictory findings have been reported in previous studies [1, 3, 8, 13, 20, 29, 30]. Latham et al [3] reported that scan patterns and IOSs were effective on the scan accuracy of complete-arch scans. This finding is in line with the findings of other studies, where the scan accuracy was affected by scan strategies [13, 30]. However, Mennito et al [29] evaluated the accuracy of sextant scans performed with different scan patterns and IOSs including the scanner utilized in the current study and revealed that scan patterns' effect was nonsignificant. Furthermore, scanning techniques were reported to be ineffective on the accuracy of complete-arch implant scans in a previous study [8]. Considering these conflicting statements, future studies are needed to elaborate the effects of scan pattern on the scan accuracy, particularly considering that CHA-SB is a relatively new system. Nevertheless, comparing the present study with abovementioned

studies [3, 8, 13, 29, 30] may be problematic due to the differences in scan patterns, the geometry of the SBs, and the anatomy of the scanned arch.

The implant at central incisor site had higher scan accuracy among the implants tested. This may be related with the maxillary arch's curvature [8], the anterior arch's linear path [8, 16, 26, 31, 32], adjacent teeth, and the morphology of the incisal or occlusal surface [33-35]. However, a careful interpretation of this finding should be made, as the current study was based on the scan accuracy of implants placed in a single quadrant without any edentulous spaces between them. In a previous study on the scan accuracy of different maxillary edentulous scenarios rehabilitated with implants (single implant, 2 implants with 1 pontic element, and 6 implants for completely edentulous maxilla), increasing the number of implants and edentulous areas was reported to decrease trueness significantly [27]. In addition, trueness of the digital scans has been reported to differ when SBs were placed in cross arches [8, 26]. Considering the novelty of the CHA-SB system in implant dentistry, multiple implants placed in different positions with larger edentulous sites should be investigated in the future.

There is limited information regarding the trueness of partially edentulous implant scans, with only 3 studies available [17-19]. A previous study [19] investigated the trueness of the scans of varied simulated SBs that were placed in 3 different sites in both quadrants performed by using 10 IOSs and reported that SB position affected the trueness. This result is in line with another study [18] performed on a similar master model. In addition, both studies showed decreased trueness further away from the starting point and attributed this finding to potential errors accumulating when image stitching [18, 19]. In another study on the trueness of the scans performed by using 2 coded healing abutments placed in 2 different sites, the premolar implant showed lower distance deviations than the molar implant [17]. However, in the present study the scans of the premolar and molar implants showed similar trueness. These contradicting results

may be related to the differences in SBs and the scanned arch. Nevertheless, the distance deviations of the present study are within the range of previous studies (13.6 to 319  $\mu\text{m}$ ) that used the same IOS (TRIOS 3) to scan single implants [18, 19, 27, 36, 37].

The accuracy of the scans of tested CHA-SB in different clinical situations was investigated in recent studies [4, 21-23]. One of those studies has investigated the effect of the operator and the implant location on the scan accuracy of the CHA-SB system, and reported that scans of the central incisor implant had higher trueness than those of premolar and molar implants [23]. In addition, contrary to the results of the present study, the scans of the molar implant showed the lowest precision in Atalay et al's [23] study. Nevertheless, a direct comparison between the present and Atalay et al's [23] studies might be misleading considering the different scan patterns utilized. In other studies, the distance deviations with the CHA-SB were reported to range from 50 to 178  $\mu\text{m}$  when a central incisor implant was digitized [4], and as 127  $\mu\text{m}$  when a mandibular first molar implant was digitized [22], which are in line with the results of the present study. However, it should be noted that present and previous studies [4, 21-23] on scan accuracy of the CHA-SB system have used complete-arch scans, which may lead to distortion of scans across the arch [38, 39] and varying deviations among different implant locations. Therefore, reported results might have been amplified and the effect of tested parameters on half-arch scans of CHA-SB should be investigated.

Three of the previous studies on the scan accuracy of CHA-SB system [21-23] have used the same methodology of the present study. In general, areas close to the top of the scan bodies are used to superimpose CAD scan body files and scan files in a CAD software. However, due to the geometry of the top of the SB, circles 3 mm below the top of the SB were used for standardization. In addition, areas towards the top of a SB are relatively easier to capture rather than areas closer to the implant platform and therefore, a circular plane closer to the top of the SB

was used to minimize line of sight related errors. Nevertheless, in another study [4], deviation of 7 points determined on 2 different planes were used to evaluate the scan accuracy of the CHA-SB system. Thus, the effect of measurement method on measured deviations may be investigated for future studies.

After the acquisition of an implant, the mesh of the SB is replaced with the corresponding library file by the dental technician [40]. Thus, an inaccuracy in the manufacturing step of the SB or an incongruence between the library file and the scanned data might lead to an inaccurate definitive prosthesis. Recent studies have reported that along with the type or geometrical design of the SB [5, 17, 20], manufacturing tolerances [2, 40], and the congruence between the SB mesh and the library CAD file [41, 42] are effective on the scan accuracy. Schmidt et al [2] studied the manufacturing tolerances of 3 SBs and showed significant differences among SBs in length, diameter, and target volume deviations. This finding was later substantiated by another study [40], where 6 different SBs were evaluated and the greatest tolerances were reported in height measurements of the implants with conical connections. Manufacturing tolerances might influence the accuracy of the scan of CHA-SB system as it consists of 2 independent pieces [4]. Donmez et al [42] evaluated the effect of IOS type on the dimensional congruence of the CHA-SB system scans when placed at mandibular right first molar site and reported a mean distance deviation of 37.8  $\mu\text{m}$  when TRIOS 3 was used. Even though the central incisor implant had a similar deviation when scanned with SP4 (36.7  $\mu\text{m}$ ), in general, higher deviations than Donmez et al's [42] study were observed in the present study. Higher deviations measured in the present study might be related to the fact that a greater surface area that comprised the entire model was aligned. The congruence between the STL file of the MRM and the library file of the CHA-SB was used to evaluate the fit between the SB and the HA in the present study. However, this analysis may also give information on the platform fit if the CAD library file is superimposed

over the acquired mesh, which should be further investigated. In addition, the effect of the assembly between the HA and the SB on scan accuracy should be investigated in future studies to elaborate the possible operator induced error on CHA-SB system scans' dimensional congruence.

The standardized in vitro design of the present study might be a limitation since the scan accuracy is affected by various factors including patient movement, gag reflex, presence of saliva or blood, and lack of space [3, 5, 8, 27]. In addition, the results of the present study are limited to a single IOS and previous studies have reported that the type [3, 7, 18, 19, 26, 27, 32, 43] and the software version [44] of an IOS affect the scan accuracy. The scans were performed by 1 experienced clinician. However, previous studies have shown the significant effect of operator experience on the scan accuracy [15, 45-48], thus the findings of the present study may differ depending on the operator. Given the fact that there is limited information regarding CHA-SB [4-10], future studies should focus on the clinical outcomes of this new system while digitizing both single and multiple implant scenarios.

## 5. CONCLUSIONS

Within the limitations of this in vitro study, the following conclusions were drawn:

1. Implant location and scan pattern influenced the scan accuracy of tested scan body combined with a healing abutment.
2. Scans performed by using SP3 had higher accuracy for all implant locations.
3. SP1 resulted in the lowest trueness for central incisor and premolar implants, while SP4 resulted in the lowest accuracy for the molar implant.
4. Central incisor implant had higher scan accuracy than those of other implants when SP4 was used.



The authors of the manuscript contributed in the following ways to the submitted manuscript:

Mustafa Borga Donmez: Drafting article, Critical revision of article

Gülce Çakmak: Design, Data collection

Sevda Atalay: Design, Data collection

Hakan Yılmaz: Data analysis, Data interpretation, Statistical analysis

Burak Yılmaz: Critical revision of the article, Approval of the submitted and final versions

#### **Declaration of interests**

The authors declare that they have no known competing financial interests or personal relationships that could have appeared to influence the work reported in this paper.

#### **Acknowledgement**

All other authors have no conflicts of interest to declare. The authors do not have any financial interest in the companies whose materials are included in this article.

Neoss Implant System is gratefully acknowledged for supplying the materials used in this study.

The authors also thank Gökhan Akcagöz for supplying the materials.

**REFERENCES**

- [1] F. Zarone, G. Ruggiero, M. Ferrari, F. Mangano, T. Joda, R. Sorrentino, Comparison of different intraoral scanning techniques on the completely edentulous maxilla: An in vitro 3-dimensional comparative analysis, *J Prosthet Dent* 124(6) (2020) 762.e1-762.e8. <http://doi.org/10.1016/j.prosdent.2020.07.017>.
- [2] A. Schmidt, J.W. Billig, M.A. Schlenz, P. Rehmann, B. Wöstmann, Influence of the accuracy of intraoral scanbodies on implant position: differences in manufacturing tolerances. *Int J Prosthodont* 32(5) (2019) 430-432. <http://doi.org/10.11607/ijp.6371>.
- [3] J. Latham, M. Ludlow, A. Mennito, A. Kelly, Z. Evans, W. Renne, Effect of scan pattern on complete-arch scans with 4 digital scanners, *J Prosthet Dent* 123(1) (2020) 85-95. <http://doi.org/10.1016/j.prosdent.2019.02.008>.
- [4] B. Yilmaz, D. Gouveia, V.R. Marques, E. Diker, M. Schimmel, S. Abou-Ayash, The accuracy of single implant scans with a healing abutment-scanpeg system compared with the scans of a scanbody and conventional impressions: an in vitro study, *J Dent* 110 (2021) 103684. <http://doi.org/10.1016/j.jdent.2021.103684>.
- [5] R.M. Mizumoto, B. Yilmaz, E.A. McGlumphy, Jr., J. Seidt, W.M. Johnston, Accuracy of different digital scanning techniques and scan bodies for complete-arch implant-supported prostheses, *J Prosthet Dent* 123(1) (2020) 96-104. <http://doi.org/10.1016/j.prosdent.2019.01.003>.
- [6] F. Mangano, A. Gandolfi, G. Luongo, S. Logozzo, Intraoral scanners in dentistry: a review of the current literature, *BMC Oral Health* 17(1) (2017) 149. <http://doi.org/10.1186/s12903-017-0442-x>.
- [7] F.G. Mangano, O. Admakin, M. Bonacina, H. Lerner, V. Rutkunas, C. Mangano, Trueness of 12 intraoral scanners in the full-arch implant impression: a comparative in vitro study, *BMC Oral Health* 20(1) (2020) 263. <http://doi.org/10.1186/s12903-020-01254-9>.
- [8] R.M. Mizumoto, G. Alp, M. Özcan, B. Yilmaz, The effect of scanning the palate and scan body position on the accuracy of complete-arch implant scans, *Clin Implant Dent Relat Res* 21(5) (2019) 987-994. <http://doi.org/10.1111/cid.12821>.
- [9] R.M. Mizumoto, B. Yilmaz, Intraoral scan bodies in implant dentistry: A systematic review, *J Prosthet Dent* 120(3) (2018) 343-352. <http://doi.org/10.1016/j.prosdent.2017.10.029>.

- [10] B. Yilmaz, S. Abou-Ayash, A digital intraoral implant scan technique using a combined healing abutment and scan body system, *J Prosthet Dent* 123(2) (2020) 206-209.  
<http://doi.org/10.1016/j.prosdent.2019.01.016>.
- [11] Vag J, Freedman G, Szabo E, Romanschky L, Berkei G. Cervical tooth anatomy considerations for prefabricated anatomic healing abutment design: A mathematical formulation, *J Prosthet Dent* (2021) <http://doi.org/10.1016/j.prosdent.2020.11.023>.
- [12] Weigl P, Trimpou G, Grizas E, Hess P, Nentwig GH, Lauer HC, Lorenz J. All-ceramic versus titanium-based implant supported restorations: Preliminary 12-months results from a randomized controlled trial, *J Adv Prosthodont* 11(1) (2019) 48-54.  
<http://doi.org/10.4047/jap.2019.11.1.48>.
- [13] L. Passos, S. Meiga, V. Brigagão, A. Street, Impact of different scanning strategies on the accuracy of two current intraoral scanning systems in complete-arch impressions: an in vitro study, *Int J Comput Dent* 22(4) (2019) 307-319.
- [14] UNI ISO 5725-1. Accuracy (trueness and precision) of measurement methods and results - part 1: General principles and definitions. Publisher: Ente Nazionale Italiano di Unificazione (UNI) (Date: 2004-01) Available at: [https://infostore.saiglobal.com/en-gb/standards/uni-iso-5725-1-2004-1099847\\_saig\\_uni\\_uni\\_2558185/](https://infostore.saiglobal.com/en-gb/standards/uni-iso-5725-1-2004-1099847_saig_uni_uni_2558185/).
- [15] C.C.D. Resende, T.A.Q. Barbosa, G.F. Moura, L.D.N. Tavares, F.A.P. Rizzante, F.M. George, F.D.D. Neves, G. Mendonça, Influence of operator experience, scanner type, and scan size on 3D scans, *J Prosthet Dent* 125(2) (2021) 294-299.  
<http://doi.org/10.1016/j.prosdent.2019.12.011>.
- [16] J. Abduo, M. Elseyoufi, Accuracy of intraoral scanners: A systematic review of influencing factors, *Eur J Prosthodont Restor Dent* 26(3) (2018) 101-121.  
[http://doi.org/10.1922/EJPRD\\_01752Abduo21](http://doi.org/10.1922/EJPRD_01752Abduo21).
- [17] B. Batak, B. Yilmaz, K. Shah, R. Rathi, M. Schimmel, L. Lang, Effect of coded healing abutment height and position on the trueness of digital intraoral implant scans, *J Prosthet Dent* 123(3) (2020) 466-472. <http://doi.org/10.1016/j.prosdent.2019.06.012>.
- [18] R.J. Kim, G.I. Benic, J.M. Park, Trueness of digital intraoral impression in reproducing multiple implant position, *PLoS One* 14(11) (2019) e0222070.  
<http://doi.org/10.1371/journal.pone.0222070>.

- [19] R.J.Y. Kim, G.I. Benic, J.M. Park, Trueness of ten intraoral scanners in determining the positions of simulated implant scan bodies, *Sci Rep* 11(1) (2021) 2606. <http://doi.org/10.1038/s41598-021-82218-z>.
- [20] C. Motel, E. Kirchner, W. Adler, M. Wichmann, R.E. Matta, Impact of different scan bodies and scan strategies on the accuracy of digital implant impressions assessed with an intraoral scanner: an in vitro study, *J Prosthodont* 29(4) (2020) 309-314. <http://doi.org/10.1111/jopr.13131>.
- [21] H. Yilmaz, H. Arinc, G. Cakmak, S. Atalay, M. B. Donmez, A. M. Kokat, B. Yilmaz, Effect of scan pattern on the scan accuracy of a combined healing abutment scan body system, *J Prosthet Dent* (2022) <http://doi.org/10.1016/j.prosdent.2022.01.018>.
- [22] G. Çakmak, M.B. Donmez, S. Atalay, H. Yilmaz, A.M. Kökat, B. Yilmaz, Accuracy of single implant scans with a combined healing abutment-scan body system and different intraoral scanners: An in vitro study, *J Dent* 113 (2021) 103773. <http://doi.org/10.1016/j.jdent.2021.103773>.
- [23] S. Atalay, G. Çakmak, M.B. Donmez, H. Yilmaz, A.M. Kökat, B. Yilmaz, Effect of implant location and operator on the accuracy of implant scans using a combined healing abutment-scan body system, *J Dent* (2021) 103855. <http://doi.org/10.1016/j.jdent.2021.103855>.
- [24] Neoss Implant System Website. [https://resources.neoss.com/uploads/11926\\_3-IFUEsthetic-Healing-Abutments-with-ScanPeg-EN-spread-PRINTINT.pdf?mtime=20210330102135](https://resources.neoss.com/uploads/11926_3-IFUEsthetic-Healing-Abutments-with-ScanPeg-EN-spread-PRINTINT.pdf?mtime=20210330102135). Accessed July 24, 2021.
- [25] GOM: ATOS Core - Features. <https://www.atos-core.com/en/features.php#3dScanning>. Accessed July 24, 2021.
- [26] G. Çakmak, H. Yilmaz, A. Treviño, A.M. Kökat, B. Yilmaz, The effect of scanner type and scan body position on the accuracy of complete-arch digital implant scans, *Clin Implant Dent Relat Res* 22(4) (2020) 533-541. <http://doi.org/10.1111/cid.12919>.
- [27] F.G. Mangano, U. Hauschild, G. Veronesi, M. Imburgia, C. Mangano, O. Admakin, Trueness and precision of 5 intraoral scanners in the impressions of single and multiple implants: a comparative in vitro study, *BMC Oral Health* 19(1) (2019) 101. <http://doi.org/10.1186/s12903-019-0792-7>.
- [28] The 3Shape Web Site <https://3shape.widen.net/view/pdf/xt7bnel76t/TRIOS-UserManual-2015-1-1.4.7.0-A-EN.pdf?t.download=true&u=6xmdhr> accessed on 21.04.2021

- [29] A.S. Mennito, Z.P. Evans, A.W. Lauer, R.B. Patel, M.E. Ludlow, W.G. Renne, Evaluation of the effect scan pattern has on the trueness and precision of six intraoral digital impression systems, *J Esthet Restor Dent* 30(2) (2018) 113-118. <http://doi.org/10.1111/jerd.12371>.
- [30] K.C. Oh, J.M. Park, H.S. Moon, Effects of scanning strategy and scanner type on the accuracy of intraoral scans: a new approach for assessing the accuracy of scanned data, *J Prosthodont* 29(6) (2020) 518-523. <http://doi.org/10.1111/jopr.13158>.
- [31] A. Ender, A. Mehl, Accuracy of complete-arch dental impressions: a new method of measuring trueness and precision, *J Prosthet Dent* 109(2) (2013) 121-8. [http://doi.org/10.1016/S0022-3913\(13\)60028-1](http://doi.org/10.1016/S0022-3913(13)60028-1).
- [32] M. Imburgia, S. Logozzo, U. Hauschild, G. Veronesi, C. Mangano, F.G. Mangano, Accuracy of four intraoral scanners in oral implantology: a comparative in vitro study, *BMC Oral Health* 17(1) (2017) 92. <http://doi.org/10.1186/s12903-017-0383-4>.
- [33] M. Braian, A. Wennerberg, Trueness and precision of 5 intraoral scanners for scanning edentulous and dentate complete-arch mandibular casts: A comparative in vitro study, *J Prosthet Dent* 122(2) (2019) 129-136.e2. <http://doi.org/10.1016/j.prosdent.2018.10.007>.
- [34] A. Ender, M. Zimmermann, A. Mehl, Accuracy of complete- and partial-arch impressions of actual intraoral scanning systems in vitro, *Int J Comput Dent* 22(1) (2019) 11-19.
- [35] K. Son, K.B. Lee, Effect of tooth types on the accuracy of dental 3D scanners: an in vitro study, *Materials (Basel)* 13(7) (2020). <http://doi.org/10.3390/ma13071744>.
- [36] L. Canullo, M. Colombo, M. Menini, P. Sorge, P. Pesce, Trueness of intraoral scanners considering operator experience and three different implant scenarios: a preliminary report, *Int J Prosthodont* 34(2) (2021) 250–253. <http://doi.org/10.11607/ijp.6224>.
- [37] B. Yilmaz, V. Rizzo Marques, X. Guo, D. Gouveia, S. Abou-Ayash, The effect of scanned area on the accuracy and time of anterior single implant scans: An in vitro study, *J Dent* 109 (2021) 103620. <http://doi.org/10.1016/j.jdent.2021.103620>.
- [38] Z. Nagy, B. Simon, A. Mennito, Z. Evans, W. Renne, J. Vág, Comparing the trueness of seven intraoral scanners and a physical impression on dentate human maxilla by a novel method, *BMC Oral Health* 20(1) (2020) 97. <http://doi.org/10.1186/s12903-020-01090-x>.
- [39] J. Vág, Z. Nagy, B. Simon, A. Mikolicz, E. Kover, A. Mennito, Z. Evans, W. Renne, A novel method for complex three-dimensional evaluation of intraoral scanner accuracy, *Int J Comput Dent* 22(3) (2019) 239-249.

- [40] H. Lerner, K. Nagy, F. Luongo, G. Luongo, O. Admakin, F.G. Mangano, Tolerances in the production of six different implant scanbodies: a comparative study. *Int J Prosthodont* 34(5) (2021) 591–599. <http://doi.org/10.11607/ijp.7379>.
- [41] F. Mangano, H. Lerner, B. Margiani, I. Solop, N. Latuta, O. Admakin, congruence between meshes and library files of implant scanbodies: an in vitro study comparing five intraoral scanners, *J Clin Med* 9(7) (2020). <http://doi.org/10.3390/jcm9072174>.
- [42] M.B. Donmez, V. R. Marques, G. Çakmak, H. Yilmaz, M. Schimmel, B. Yilmaz, Congruence between the meshes of a combined healing abutment-scan body system acquired with four different intraoral scanners and the corresponding library file: An in vitro analysis, *J Dent* 118 (2022) 103938. <http://doi.org/10.1016/j.jdent.2021.103938>.
- [43] F.G. Mangano, G. Veronesi, U. Hauschild, E. Mijiritsky, C. Mangano, Trueness and precision of four intraoral scanners in oral implantology: a comparative in vitro study, *PLoS One* 11(9) (2016) e0163107. <http://doi.org/10.1371/journal.pone.0163107>.
- [44] J. Vág, W. Renne, G. Revell, M. Ludlow, A. Mennito, S.T. Teich, Z. Gutmacher, The effect of software updates on the trueness and precision of intraoral scanners, *Quintessence Int* 52(7) (2021) 636-644. <http://doi.org/10.3290/j.qi.b1098315>.
- [45] B. Giménez, M. Özcan, F. Martínez-Rus, G. Pradíes, Accuracy of a digital impression system based on parallel confocal laser technology for implants with consideration of operator experience and implant angulation and depth, *Int J Oral Maxillofac Implants* 29(4) (2014) 853-62. <http://doi.org/10.11607/jomi.3343>.
- [46] B. Giménez, M. Özcan, F. Martínez-Rus, G. Pradíes, Accuracy of a digital impression system based on active triangulation technology with blue light for implants: effect of clinically relevant parameters, *Implant Dent* 24(5) (2015) 498-504. <http://doi.org/10.1097/ID.0000000000000283>.
- [47] G. Revell, B. Simon, A. Mennito, Z.P. Evans, W. Renne, M. Ludlow, J. Vág, Evaluation of complete-arch implant scanning with 5 different intraoral scanners in terms of trueness and operator experience, *J Prosthet Dent* (2021). <http://doi.org/10.1016/j.prosdent.2021.01.013>.
- [48] M. Schimmel, N. Akino, M. Srinivasan, J.G. Wittneben, B. Yilmaz, S. Abou-Ayash, Accuracy of intraoral scanning in completely and partially edentulous maxillary and mandibular jaws: an in vitro analysis, *Clin Oral Investig* 25(4) (2021) 1839-1847. <http://doi.org/10.1007/s00784-020-03486-z>.

## TABLES

**Table 1.** Two-way ANOVA results of the deviation measurements

<b>Property</b>	<b>Effect</b>	<b>df</b>	<b>F Ratio</b>	<b>P value</b>
	Scan Pattern	3	19,865	<.001
Distance Deviation ( $\mu\text{m}$ ) (Trueness)	Implant Location	2	12,665	<.001
	Scan Pattern * Implant Location	6	4,383	.001
	Scan Pattern	3	2,714	.05
Distance Deviation ( $\mu\text{m}$ ) (Precision)	Implant Location	2	2,230	.114
	Scan Pattern * Implant Location	6	2,738	.018
	Scan Pattern	3	2,714	.05

**Table 2.** Mean  $\pm$ standard deviation values for distance deviation (trueness) and 95% confidence

Scan Pattern	Implant Position		
	Molar	Premolar	Central Incisor
SP1	124.7 $\pm$ 37.9 <sup>abA</sup> (93.1-156.4)	158 $\pm$ 39.5 <sup>bA</sup> (125-191)	123.5 $\pm$ 57.8 <sup>bA</sup> (75.2-171.8)
SP2	71.9 $\pm$ 25.7 <sup>aAB</sup> (50.4-93.4)	94.1 $\pm$ 20.4 <sup>aB</sup> (77.1-111.1)	56.7 $\pm$ 35.9 <sup>aA</sup> (26.6-86.7)
SP3	75.4 $\pm$ 37.9 <sup>aA</sup> (43.7-107.1)	63.2 $\pm$ 27.3 <sup>aA</sup> (40.4-86)	46.7 $\pm$ 31.3 <sup>aA</sup> (20.5-72.9)
SP4	147.2 $\pm$ 49.7 <sup>bc</sup> (105.7-188.8)	100.3 $\pm$ 20 <sup>aB</sup> (83.6-117)	36.2 $\pm$ 18.6 <sup>aA</sup> (20.6-51.8)

limits for each scan pattern-implant location pair

\*Different lowercase letters in same column and different uppercase letters in same row indicate significant differences ( $P < .05$ ).



**Table 3.** Mean  $\pm$ standard deviation values for distance deviation (precision) and 95% confidence limits for each scan pattern-implant location pair

Scan Pattern	Implant Position		
	Molar	Premolar	Central Incisor
SP1	29.1 $\pm$ 21.6 <sup>aA</sup> (11-47.2)	29.3 $\pm$ 24.1 <sup>aA</sup> (9.1-49.4)	47.7 $\pm$ 27 <sup>bA</sup> (25.2-70.3)
SP2	15.4 $\pm$ 19.8 <sup>aA</sup> (-1.1-31.9)	17.2 $\pm$ 8.7 <sup>aA</sup> (9.9-24.5)	31.1 $\pm$ 13.6 <sup>abA</sup> (19.8-42.4)
SP3	27 $\pm$ 24.6 <sup>aA</sup> (6.4-47.6)	18.8 $\pm$ 18.5 <sup>aA</sup> (3.3-34.2)	23.4 $\pm$ 18.8 <sup>abA</sup> (7.7-39.1)
SP4	43 $\pm$ 18.9 <sup>ab</sup> (27.1-58.8)	15.4 $\pm$ 11.3 <sup>aA</sup> (5.9-24.9)	14.1 $\pm$ 11 <sup>aA</sup> (4.9-23.3)

\*Different lowercase letters in same column and different uppercase letters in same row indicate significant differences ( $P < .05$ ).

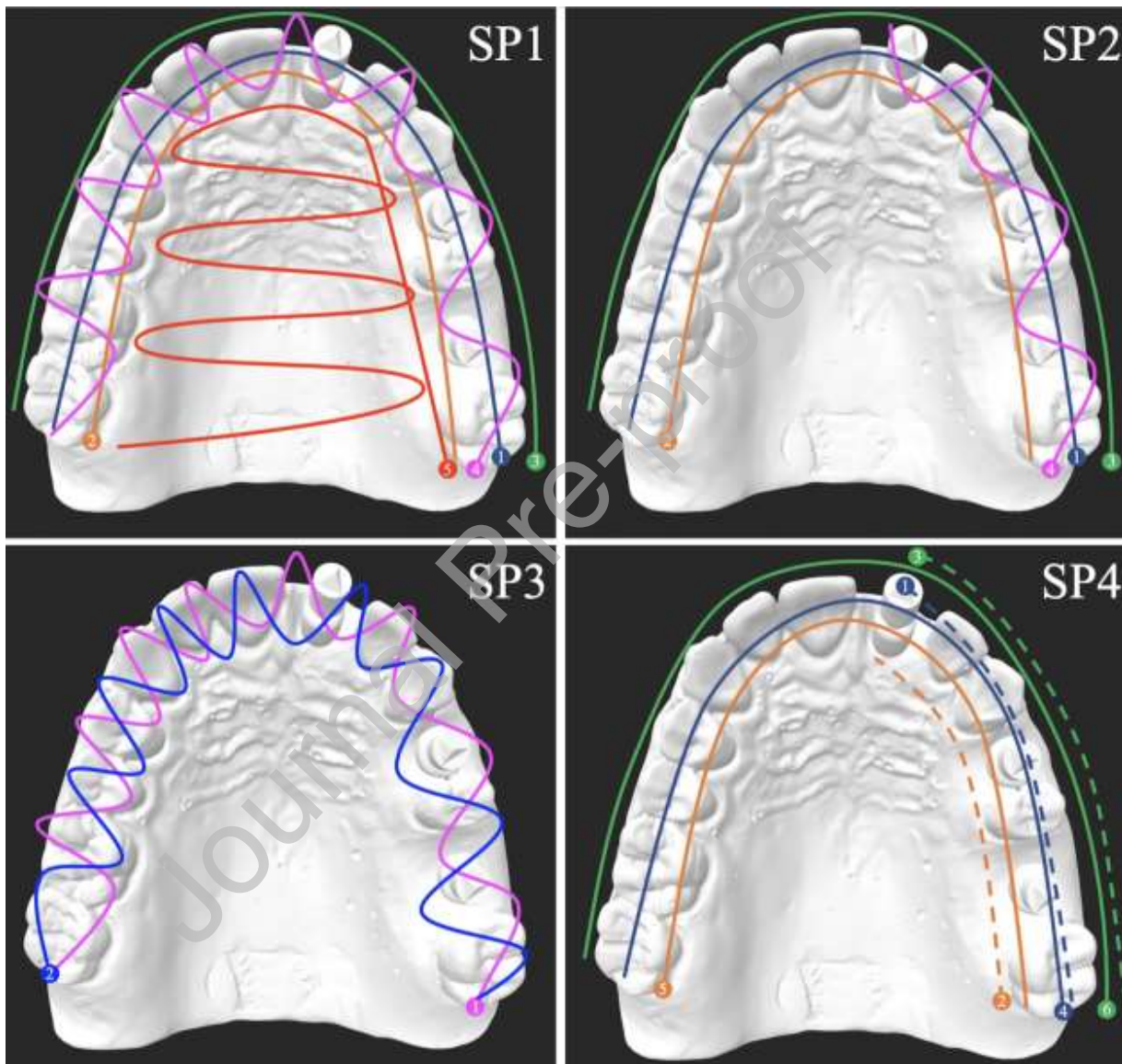
**Figure Legends**

**Figure 1.** Scan Peg, healing abutment, and assembled combined healing abutment-scan body

system



**Figure 2.** Scan patterns used in present study (Navy blue: Occlusal scan; Orange: Lingual scan; Green: Buccal scan; Pink: Buccolingual rotational movement; Blue: Reverse buccolingual rotational movement; Red: Sweeping motion of palate; Starting point of each movement is shown



with numbered dots)

**Figure 3.** Planes (A) and circles (B) generated in nominal and test scans for measurement of distance deviations (C)

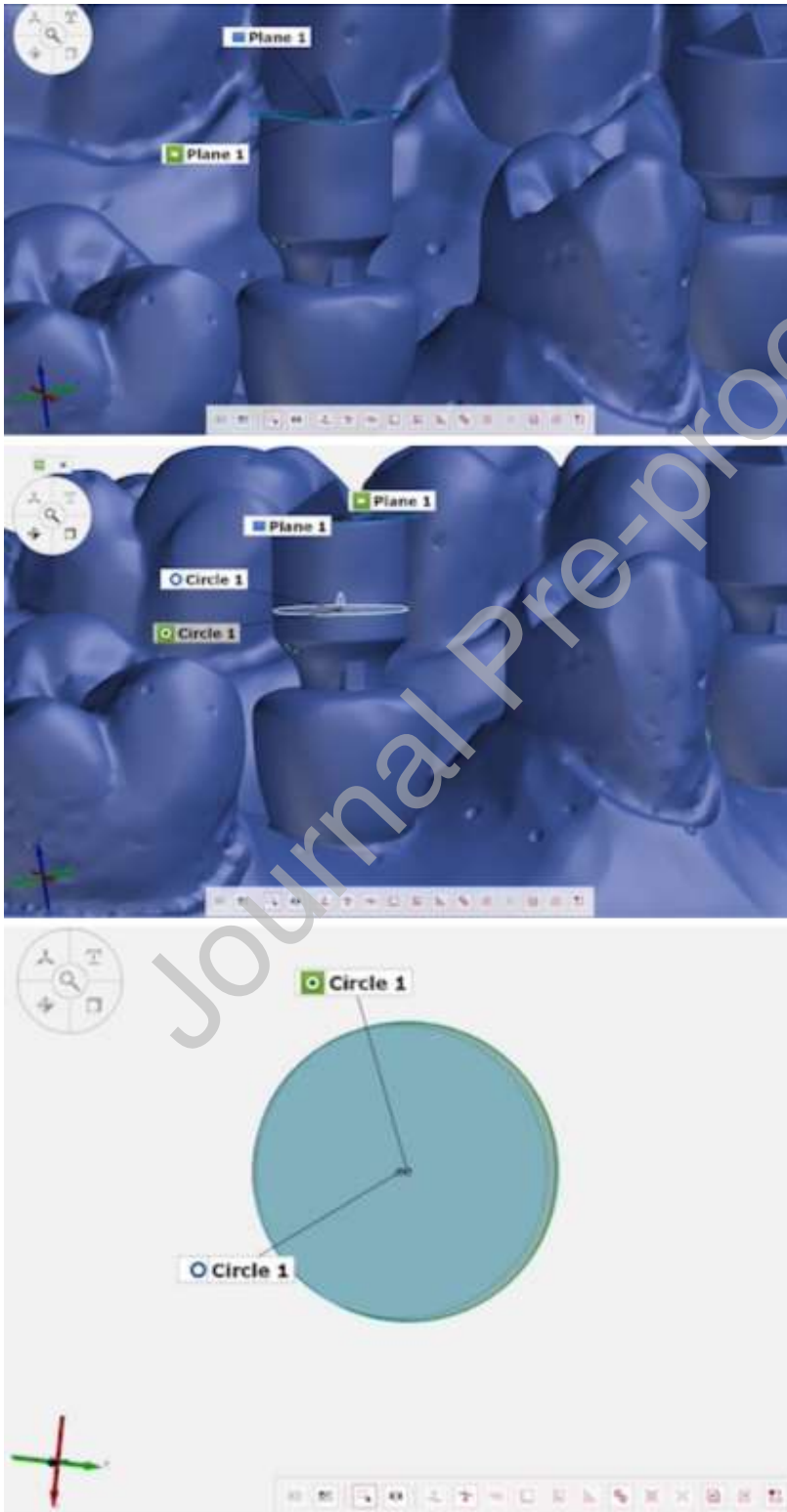


**Figure 4.** Maximum distance deviation of the master model mesh when superimposed over the library CAD file for each implant position

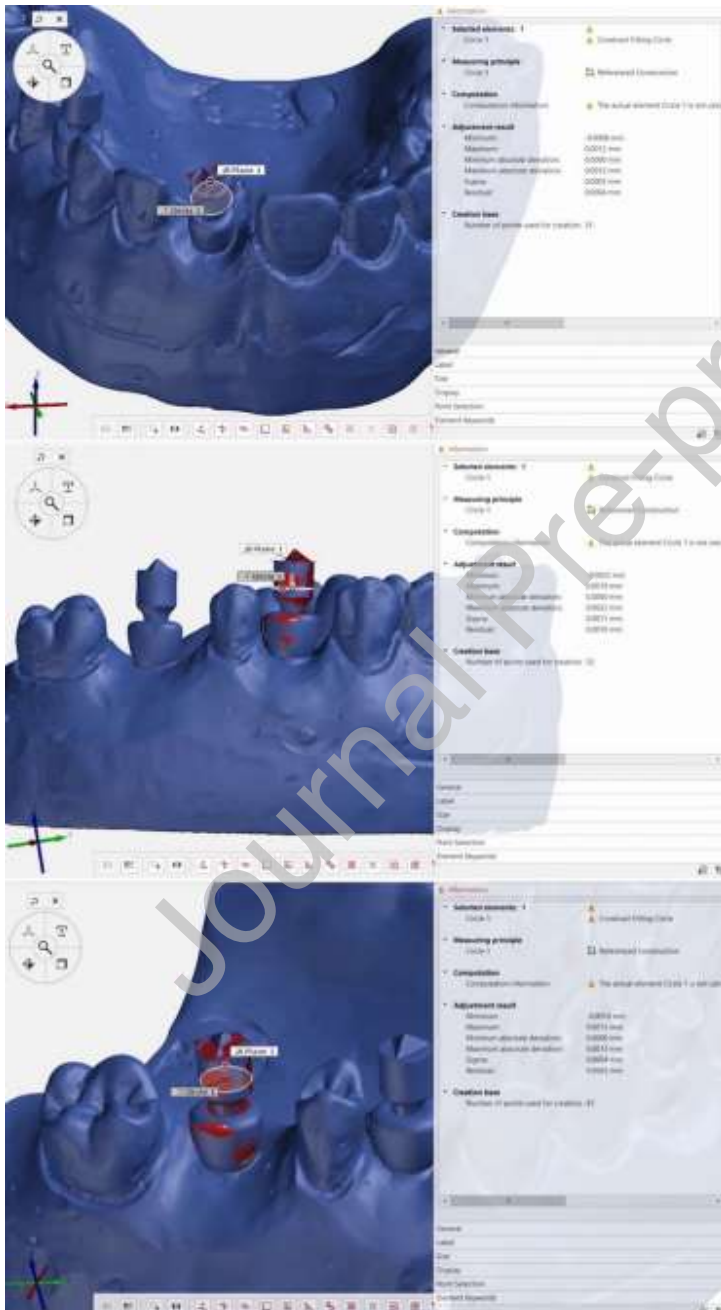


**Figure 5.** Means and 95% confidence intervals (error bars) of distance deviations for each scan pattern-implant location pair

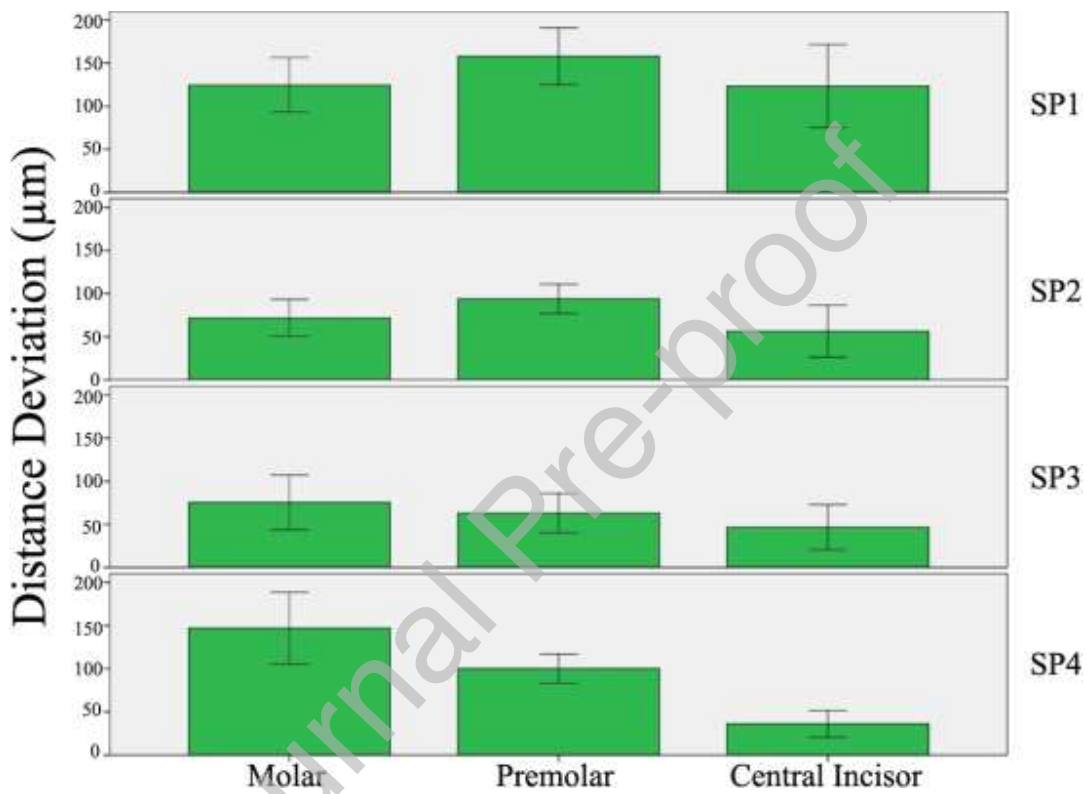


**Figure 6.** Means and 95% confidence intervals (error bars) of precision of distance deviations for each scan pattern-implant location pair

